Anti-tumor effects of anti-Semaphorin 4D antibody unravel a novel pro-invasive mechanism of vascular targeting agents

Iratxe Zuazo-Gaztelu[1*], Marta Pàez-Ribes[1*], Patricia Carrasco[1*], Laura Martín[1*], Adriana Soler[2], Mar Martínez-Lozano[1], Roser Pons[1], Judith Llena[2], Luis Palomero[1], Mariona Graupera[2] and Oriol Casanovas[1#].

[1] Tumor Angiogenesis Group, ProCURE Research Program – Catalan Institute of Oncology, OncoBell Program – IDIBELL, Spain.
[2] Vascular Signaling Group, ProCURE Research Program – IDIBELL, Spain.
* Contributed equally.

Running title: Induction of tumor aggressivity after anti-Sema4D treatment

Keywords: Tumor angiogenesis, RIP1-Tag2, Semaphorin 4D, macrophages, SDF1.

Additional information:

Financial support: This work is supported by research grants from ERC (ERC-StG-281830) EU-FP7, MinECO (SAF2016-79347-R), ISCIII Spain (AES, DTS17/00194) and AGAUR-Generalitat de Catalunya (2017SGR771). Some of these include European Development Regional Funds (ERDF “a way to achieve Europe”). Vaccinex Inc. provided reagents and research money (<20.000 Eur) to support this work.

[#], Corresponding author: Oriol Casanovas.
Tumor Angiogenesis Group. ProCURE Research Program, Catalan Institute of Oncology – OncoBell Program, IDIBELL. Av. Gran Via 199-203 (3a pl). 08908-L’Hospitalet de Llobregat, Spain. Phone: +34-932607344, Fax: +34-932607466. ocasanovas@iconcologia.net

Conflict of interest: Vaccinex Inc. provided reagents and research money (<20.000Eur) to support this work. Other autors declare no conflicts of interest.

Word count: 5.116 words (without abstract and references) and 44 references

Total number of figures and Tables: 7 figures

ABSTRACT

One of the main consequences of inhibition of neovessel growth and vessel pruning produced by angiogenesis inhibitors is increased intratumor hypoxia. Growing evidence indicates that tumor cells escape from this hypoxic environment to better nourished locations, presenting hypoxia as a positive stimulus for invasion. In particular, anti-VEGF/R therapies produce hypoxia-induced invasion and metastasis in a spontaneous mouse model of pancreatic neuroendocrine cancer (PanNET), RIP1-Tag2. Here, a novel vascular targeting agent targeting Semaphorin 4D (Sema4D) demonstrated impaired tumor growth and extended survival in the RIP1-Tag2 model. Surprisingly, although there was no induction of intratumor hypoxia by anti-Sema4D therapy, the increase in local invasion and distant metastases were comparable with the ones produced by VEGFR inhibition. Mechanistically, the antitumor effect was due to an alteration in vascular function by modification of pericyte coverage involving PDGF-B. On the other hand, the aggressive phenotype involved a macrophage-derived Sema4D signaling engagement which induced their recruitment to the tumor invasive fronts and secretion of stromal derived factor 1 (SDF1) that triggered tumor cell invasive behavior via CXCR4. A comprehensive clinical validation of the targets in different stages of PanNETs demonstrated the implication of both Sema4D and CXCR4 in tumor progression. Taken together, we demonstrate beneficial anti-tumor and pro-survival effects of anti-Sema4D antibody but also unravel a novel mechanism of tumor aggressivity. This mechanism implicates recruitment of Sema4D positive macrophages to invasive fronts and their secretion of pro-invasive molecules that ultimately induce local tumor invasion and distant metastasis in PanNETs.

INTRODUCTION

One of the main consequences of vessel pruning and inhibition of neovessel growth produced by angiogenesis inhibitors is the increased hypoxia levels produced inside the tumors. Cancer cells can live in hypoxic conditions (1), but growing evidence indicates that tumor cells may escape from this hypoxic environment to better nourished locations, presenting hypoxia as a positive stimulus for invasion (2). In fact, a strong correlation among tumor hypoxia and increased invasion, metastasis and poor patient outcome has been reported (3–5). In this context, alternative angiogenic targets such as semaphorins are beeing explored (6).

Semaphorins (SEMAs) are a superfamily of secreted or membrane-associated glycoproteins implicated in axonal wiring control, angiogenesis and cancer progression. Semaphorin 4D (Sema4D) is a transmembrane protein of 150 KDa of the IV class of the subfamily of semaphorins involved in the regulation of axon guidance, cell migration in organ development and vascular morphogenesis (7–9). Three receptors are known for Sema4D: high-affinity receptor Plexin-B1 (PlxnB1), expressed in a wide variety of cell types, intermediate affinity Plexin-B2 (PlxnB2), and low-affinity receptor, CD72, mainly expressed in cells of the immune system (10,11). Sema4D is highly expressed in the membrane of most frequent solid tumors, including breast, prostate and colon (12), and also in tumor associated macrophages (TAMs), with a relevant role in tumor invasion, angiogenesis and metastasis (13). High expression levels of Sema4D have been also reported in tumor stroma (14). Due to proteolytical cleavage

by matrix metalloproteinase type 1 (MT1-MMP, also known as MMP14) a Sema4D soluble form is released (15,16), allowing to act through PlxnB1 on endothelial cells and promoting angiogenesis which permits tumors to be nourished with the necessary nutrients and oxygen to continue its growth (12). In fact, there is a completed Phase I clinical trial to evaluate the safety and tolerability of intra-venous (IV) administration of an antibody anti-Sema4D VX15/2503 (Vaccinex Inc, Rochester, NY) in patients with advanced solid tumors (ClinicalTrials.gov identifier: NCT01313065) (17).

In this study, using a spontaneous mouse model of pancreatic neuroendocrine cancer (PanNET), RIP1-Tag2 mice, we describe alteration of tumor vascular function by the use of a vascular-targeting agent anti-Sema4D antibody that consequently impairs tumor growth. Unlike VEGF/R blockade, induction of intratumor hypoxia is not observed after anti-Sema4D therapy, but the increase in local invasion and distant metastases are comparable with anti-VEGFR2's effects. This hypoxia-independent mechanism of increased aggressive phenotype is associated with recruitment of TAMs as mediators of increased invasion and dissemination of tumor cells after anti-Sema4D treatment. Mechanistically, anti-Sema4D antibody induces a Sema4D signaling engagement in the membrane of macrophages not only for their motility and recruitment to the tumor invasive fronts, but also for increased secretion of stromal derived factor 1 (SDF1). In turn, SDF1 enhances tumor cell invasive behavior via CXCR4 and triggers the malignant PanNET phenotype in anti-Sema4D treated RIP1-Tag2 mice. Finally, we also present clinical evidence that support a role for Sema4D and SDF1 overexpression in human macrophages and an association of Sema4D and CXCR4 in PanNETpatients tumor progression.

MATERIALS AND METHODS

Animal model and Therapeutic Trials

Transgenic RIP1-Tag2 mice have been previously reported (18). Animal housing, handling and all procedures were approved by our institution's ethical committee and Government committees. Tumor volume, type, invasiveness and hemorrhagic phenotype was determined as previously described (19). Four week-long treatments in RIP1-Tag2 mice started at 12 weeks of age with: 1) Anti-Semaphorin 4D Mab67 function blocking murine IgG1 antibody (anti-Sema4D) kindly provided by Vaccinex Inc, Rochester, NY (20), 2) anti-VEGFR2 blocking antibody (DC101) purified in our laboratory or 3) ChromPure Mouse IgG1 whole molecule as isotype control (Jackson Immuno Research Laboratories, Inc). All dosed at 1mg/animal once a week IP except for anti-VEGFR2 which was administered twice-a-week as previously described (21).

Histological analyses and quantification

Frozen or paraffin samples of Pancreata and livers were histologically evaluated with primary antibodies: anti-CD31 (550274; 1:50; BD Biosciences); anti-T-antigen (1:10000; Hanahan laboratory), anti-Hypoxyprobe (1:50; NPI Inc), anti-GLUT1 (ab652; 1:100; Abcam), anti-Type IV Collagen (AB756P; 1:200; Millipore), anti-Lyve1 (103-PA50AG; 1:100; ReliaTech), anti-Desmin (ab15200; 1:150; Abcam), anti-NG2 (AB5320; 1:50; Millipore), anti-SMA-Cy3 (C6198; 1:200; Sigma-Aldrich), anti-SMA (RB-9010; 1:100; Thermo Scientific), anti-PlxnB1 (sc-28372; 1:50; Santa Cruz Biotechnology), anti-Sema4D (G3256; 2 µg/mL; Vaccinex company), anti-F4/80 (MCA497R; 1:50; AbD Serotec), anti-CD3e (550275; 1:10; BD Bioscience), anti-CD72 (PAB261Mu01; 1:100; Cloud-clone Corp), anti-SDF1 (MAB350, 1:20, R&B System),

anti-CXCR4 (C8352, 1:750, Sigma), and anti-Insulin (A0564; 1:50; Dako). Microvessel density, pericyte coverage of tumor vessels, macrophage infiltration, CXCR4, SDF1 and Sema4D expression were manually quantified per field. Collagen IV, VE-cadherin and tumor hypoxia were measured as the mean positive area per field.

Cell culture and conditioned media obtention

βTC4 cell line was isolated from RIP1-Tag2 tumors in Hanahan laboratory and grown in DMEM 20% FBS. To discard undifferentiation events, they were not used beyond 50 passages and their phenotype was authenticated by insulin expression by immunocytofluorescence. RAW264.7 cell line, donated by E. Ballestar (IDIBELL), was grown in DMEM 10% FBS and THP-1 cells, donated by I. Fabregat (IDIBELL), were grown in RPMI 10% FBS. These had been bought by ATCC and authenticated by STR profiling by the ATCC. HUVEC cells from CellTech (Spain) were grown in EGM/EBM2 10% iFBS. All cell lines were examined for mycoplasma contamination using PCR analysis every month. For conditioned media: RAW264.7, HUVEC and THP-1 cells were grown in free-serum DMEM and treated with anti-Sema4D (10 μg/mL), either Vaccinex (Mab67) or Abnova (3B4), isotype-specific anti-IgG1 (10 μg/mL, isotype control), or without treatment (control) during 24h. RAW264.7 cells were also treated with recombinant Sema4D (5235-S4-050 and PlxnB2 (6836-PB-050) at 1 μg/mL (R&D systems). In added conditioned media the antibodies were added after media collection.

Generation of shRNA RAW264.7 clones

shRNAs designed by The RNAi Consortium (TRC) cloned into the pLKO.1 lentiviral vector were purchased from Dharmacon (GE Healthcare) for silencing of Sema4D (TRCN0000067493), CD72 (TRCN0000066042), Plxnb2 (TRCN0000078853) and non-targeting shRNA (shNS) as a negative control. shRNA lentivirus were used to transduce RAW264.7 cells with 8 μg/ml polybrene and after 48h selected with 1 μg/mL puromycin for 5 days.

Migration and matrigel invasion transwell assays

Corning migration and invasion assays (#3422 & #354480) were performed following manufacturer's instructions. RAW264.7 and THP-1 cells were treated with anti-Sema4D (10 μg/mL), either Vaccinex (Mab 67) or Abnova (3B4), isotype-specific IgG1 (10 μg/mL) or without treatment. βTC4 cells in serum-free DMEM media were subjected to RAW264.7 conditioned media. For chemotaxis assay for SDF1, treatments included 1 μg/ml AMD3100 (3299, Tocris) and 100 ng/ml recombinant SDF1 (250-20A, Peprotech).

Protein analysis and RNA Analysis

Tumor samples and βTC4 and RAW264.7 cell lysates were analyzed by WB with: c-met (sc-8057; 1:100; Santa Cruz Biotech.), phospho-c-met (3077; 1:750; Cell Signaling), PlxnB2 (AF5329; 1:1000; R&D), Sema4D (MAB5235; 1:250; Novus Biologicals), CD72 (AF1279; 1:500; R&D), α-tubulin (32-2500; 1:2000; Invitrogen). For mRNA, RNA extraction and High-Capacity RT reaction (Applied Biosystems) produced cDNA for RT-PCR using LDA Arrays for 24 genes (Supplementary Table 1) and SDF1 and CXCR4, HPRT1 (mouse and human), and cMET and β-ACTIN (mouse) Taqman probes (Applied Biosystems).

Cytokine Array and ELISA

Supernatants of RAW264.7 conditioned media were analyzed by mouse cytokine antibody array (#AAM-CYT-1000; RayBiotech, Inc.) according to the manufacturer's instructions. Mouse SDF1 ELISA (MCX120, R&D) was performed after concentrating supernatants with Vivaspin 2 KDa column (Sartorius). Similarly, human SDF1 ELISA (DSA00; R&D) was done in supernatants of HUVEC and THP-1 conditioned media.

Mouse Omics and Clinical data analysis

Gene expression data from different stages of RIP1-Tag2 mice (GEO Omnibus ID – GSE73514) and human mRNA transcriptomes from a core independent clinical gene expression dataset of PanNET (GEO Omnibus ID – GSE73338) patients were used (22,23). For RIP1-Tag2 mice data, primary tumors (n=5) and metastases (n=3) samples were compared. For the human study, normal pancreatic islet samples (n=4), nonfunctional samples (n=63), which were termed primary tumors, and their corresponding metastases (n=7) were evaluated. To further study the malignization process, primary tumors were divided into two subcategories, non-malignant and malignant, according to the clinical history of the patients (23).

Statistical Analysis

Results are presented as mean ± SD, except for transwell assays, which results are presented as mean ± SEM. The statistical tests are noted in each figure and significance follows * $p<0.05$, ** $p<0.005$, *** $p<0.001$, **** $p<0.00001$ consensus.

RESULTS

Treatment with anti-Sema4D exerts an antitumor and prosurvival effect

Initially, the presence of Sema4D and its high affinity receptor PlxnB1 was evaluated. Sema4D was found to be highly expressed in the membrane of scattered single cells inside tumor parenchyma with a pattern compatible with immune cells and weakly expressed in the membrane of tumor cells (Supplementary Figure 1A), consistent with previous reports (15,17). PlxnB1 was immunodetected in a 30% of vascular structures (Supplementary Figure 1B). To assess the effects of anti-Sema4D treatment, we used a specific antibody (anti-Sema4D, Mab67 Vaccinex) (20) in RIP1-Tag2 mice and focused on tumor growth and expansion phase of islet carcinoma. Therapeutical regimes included 2 or 4 weeks anti-Sema4D treatment along with treatment with DC101, a well described blocking monoclonal antibody of VEGFR2 (21). We could determine that 4 weeks therapy produced an inhibition in tumor growth similar to the one observed after anti-VEGFR2 (α-VR2) treatment (Figure 1A), which promoted an extension of lifespan of treated mice (Figure 1B). These results suggest an anti-tumor benefit of anti-Sema4D therapy in terms of tumor shrinkage and lifespan increase in mice.

Altered vessel structure and functionality

A qPCR for angiogenesis related genes such as angiopoietins and platelet-derived growth factor receptors was modified after the treatment (Supplementary Table 1). Suprisingly, in contrast to differences observed after anti-VEGFR2, treatment with anti-Sema4D did not show any differences in number of vessel structures (Figure 1C; Supplementary Figure 1C top) or CD31 area density (Figure 1D) nor matrix deposition of endothelial cells determined using type IV collagen (Figure 1E; Supplementary Figure 1C middle). Moreover, there was no difference in area and structure of endothelial cell-cell junctions, as shown by VE-cadherin evaluation (Figure 1F, Supplementary Figure 1C bottom), in contrast to the significant alterations observed after anti-VEGFR2 therapy. Other vascular parameters such as number of branches and empty sleeves did not show any differences either (Supplementary Figure 1D-E). Lymphangiogenesis was also evaluated, observing no lymphangiogenic events neither in the control nor in the anti-Sema4D treated condition (Supplementary Figure 2A).

Together, these data indicate that anti-Sema4D treatment does not produce a classical anti-angiogenic effect at the endothelial level on RIP1-Tag2 model. To mechanistically understand why anti-Sema4D does not exert a direct anti-angiogenic effect, we evaluated the presence of membrane-bound or soluble Sema4D forms in our model. As shown in Supplementary Figure 2B, in RIP-Tag2 tumors we can only detect Sema4D transmembrane full-length form (150 KDa) and not detect any soluble form (110-115 KDa). As the soluble form has been associated to angiogenesis, the lack of this soluble form is consistent with a lack of antiangiogenic effects of anti-Sema4D.

Since many other cellular types such as pericytes play fundamental structural and functional roles in blood vessels, pericyte coverage was evaluated to determine whether they were subjected to a further structural change after anti-Sema4D therapy. Pericytes positive for Desmin and NG2 were increased after anti-Sema4D treatment whereas the number of α-SMA positive pericytes was decreased (Figure 1G; Supplementary Figure 3A). This alteration in pericyte profile suggests a switch to a more immature vessel type associated to vascular remodeling. In addition, after anti-Sema4D therapy there is a nearly two-fold increase in the number of PlxnB1 positive structures (Supplementary Figure 3B). Next, we checked whether these changes in pericyte coverage occur in PlxnB1 possitive vessels (Supplementary Figure 3C). No difference in pericyte coverage between the PlxnB1 positive or negative endothelial cells was observed, evidencing that pericyte coverage is independent from the expression of PlxnB1 in endothelial cells. This suggests an indirect crosstalk between endothelial cells and pericytes.

Based on previous work (24), where Sema4D treatment of endothelial cells elicits production of PDGF-BB and promotes differentiation of mesenchymal stem cells into pericytes, thus producing pericyte proliferation, chemotaxis, and association with HUVECs in a capillary network, we checked PDGF-BB expression. ELISA assay of PDGF-BB showed a slight decrease in PDGF-BB levels in α-Sema4D treated tumors when compared to control tumors (Supplementary Figure 4). This result was concordant with our RNA analysis in which a decrease in PDGF-BB levels was also observed (Supplementary Table 1).

To assess if altered pericyte coverage after anti-Sema4D had further consequences in vascular functionality, we checked vascular integrity. We evaluated a vascular leakage parameter such as extravassation of erithrocytes (microhemorrhaging) in the form of tumor hemorrhagic phenotype. The percentage of hemorrhagic tumors after 2 weeks of anti-Sema4D therapy was significantly reduced when compared to control animals, although this reduction was even stronger with anti-VEGFR2 treatment (Figure 1H; Supplementary Figure 5A left). These effects were maintained in long term treatment (Supplementary Figure 5A right). Aiming at identifying other possible causes of the change in pericyte coverage after anti-Sema4D treatment, we screened for CD72 low affinity receptor presence in pericytes from tumor vasculature. We could determine that CD72 is not expressed in vascular nor perivascular cells (Supplementary Figure 5B). CD72 was rather found to be expressed in single cells, suggestive of its expression in cells of the immune system infiltrated in tumor stroma (Supplementary Figure 5C). This result is further confirmed by a double costaining of CD72 and F4/80 positive macrophages (Supplementary Figure 5D).

Increased invasiveness and metastasis after anti-Semaphorin 4D treatment

Anti-Sema4D treatment increases the number of highly invasive tumors progressively, similar to the effect of anti-VEGFR2 (Figure 2A and B). While the majority of control tumors were predominantly encapsulated or microinvasive, treated tumors presented wide fronts of invasion encroaching into adjacent acinar tissue. Significantly, this effect was further exacerbated when anti-Sema4D therapy was maintained for 4 continuous weeks (Figure 2B). Study of livers and peripancreatic lymph nodes (LN) revealed that anti-Sema4D treated mice more frequently contained enlarged LN containing tumor cells and distant metastasis to the liver (Figure 2C). The incidence of LN metastasis grew from the 30% in untreated controls to more than 70% in treated groups, indicating that similarly to what happens with VEGFR2 inhibition, anti-Sema4D treatment promotes an increase in LN metastasis (Figure 2D, left). Incidence of liver metastasis was 2-fold higher in those mice that had received an antiangiogenic treatment, either anti-VEGFR2 or anti-Sema4D (Figure 2D, right). When combining anti-Sema4D and anti-VEGFR2, results in tumor burden, survival, invasiveness and metastases incidence were identical as in anti-VEGFR2 alone (Supplementary Figure 6). This lack of additional effectof anti-Sema4D evidences the predominant role of VEGF in triggering angiogenesis over Sema4D in this tumor setting.

Overall, the data presented here demonstrate that anti-Sema4D treatment promotes the acquisition of an adaptive resistance, with similar effects of the complete and lasting inhibition of angiogenesis caused by the use of anti-VEGFR2 or TK inhibitors as sunitinib and sorafenib (19,25).

Malignization after anti-Sema4D treatment is not produced by known mechanisms

Treatments targeting tumor vasculature are described to produce an increase in hypoxia as a consequence of the antiangiogenic effect. Surprisingly, anti-Sema4D treatment did not induce hypoxia in short-term treated tumors, as demonstrated by the presence of pimonidazole adducts or by the increase in the expression of hypoxia-response genes such as Glut1 (Figure 3A) in anti-VEGFR2 treated tumors. Quantification of this event at longer treatment regimes confirmed this observation (Figure 3B-C). Taken together, these data suggest that a hypoxia independent pathway is responsible for the increase in invasion and malignization.

Up to now, the best described mechanism of tumor aggressiveness after anti-vascular inhibition in RIP1-Tag2 tumors involves hypoxia and c-met activation (26,27). RNA analysis of untreated and anti-Sema4D treated tumors revealed that there were no changes in c-met expression (Figure 3D). We then assayed the presence of its precursor protein and its active form, phosphorylated c-met, by western blotting, using HGF (c-met natural ligand) to stimulate cells. No expression of the precursor and any activation of c-met signaling pathway was observed, neither in the untreated nor in the anti-Sema4D treated conditions (Figure 3E). Similarly, even if βTC4 cells express c-met at low transcriptional levels, there is no pathway activation in response to anti-Sema4D or HGF (Figure 3F-G). Overall, these data suggest that malignization effects in RIP1-Tag2 mice are restricted to an indirect effect of Sema4D over tumor cells, rather than to a direct action of the pro-angiogenic molecule upon tumor cell derived c-

met. Moreover, a retrograde effect of Sema4D over tumor cells was discarded since no changes in cell adhesion, de-adhesion or proliferation of RIP1-Tag2-derived βTC4 tumor cells were observed (Supplementary Figure 7).

Anti-Sema4D treatment produces an increase in tumor-associated macrophage (TAM) migration

Among all immune cells expressing Sema4D (28–31), a relevant role in pro-tumorigenic processes has been specifically described for lymphocytes and TAMs (13,14). CD3e-positive T-lymphocytes infiltrated in the RIP-Tag2 tumor parenchyma were very scarce and, while anti-Sema4D treatment produced an increase in their numbers, the absolute amount was too low to consider them functionally relevant (Supplementary Figure 8). On the other hand, a co-staining of macrophage marker F4/80 with Sema4D in our tumors showed that most macrophages did not express Sema4D, few expressed it with high intensity and some only in certain areas of the cell (Figure 4A). However, we found a visible higher amount of Sema4D positive macrophages after anti-Sema4D therapy (Figure 4A) and the total number of macrophages was significantly increased (Figure 4B). In fact, while the number of Sema4D negative macrophages was maintained invariable after the therapy (Figure 4C), the number and percent of Sema4D positive macrophages increased after short term anti-Sema4D treatment (Figure 4D). In conjuction, these data demonstrated that, *in vivo*, there was a change in the number and phenotype of TAMs after anti-Sema4D treatment. In order to functionally validate its consequences, the migration properties of a Sema4D-expressing murine macrophage cell line, RAW264.7 (Supplementary Figure 9A), were evaluated after anti-Sema4D treatment. As shown in Figure 4E, there was an increase in migration of RAW264.7 cells after anti-Sema4D therapy, which occurred in a dose dependent manner (Supplementary Figure 9B). Moreover, the addition of exogenous recombinant Sema4D did not reduce basal macrophage migration, indicating the requirement for Sema4D expression in cell membrane for the antibody to have an effect (Figure 4E). To decipher the underlying mechanism, effective knockdowns of the ligand Sema4D and its two receptors expressed in RAW264.7 cells, CD72 and PlxnB2 were generated (Supplementary Figure 9C). Interestingly, we observed that there was no change in migratory capacity of RAW264.7 cells in any of the gene knockdowns (Figure 4F). Moreover, anti-Sema4D treatment continued to produce the same increase of migration in all gene silencing conditions except for shSema4D cells (Figure 4G; Supplementary Figure 9D). Altogether, our results define a receptor-independent and Sema4D-requirement for antibody induction of migration and they demonstrate that Sema4D needs to be expressed in the membrane of the cells for the antibody to have an effect. Thus, all these data define an antibody-induced retrograde signaling engagement of Sema4D which has already been previously published for this family of transmembrane proteins in different settings (reviewed in 32 and 33).

Most macrophage activity is mediated by cytokines and chemokines that act in autocrine fashion and paracrine fashion, upon other macrophages or even upon other cells from the tumor ecosystem. Aiming to delve into macrophage study, we performed a mass spectrometric analysis (LC-MS/MS) of secreted proteins (secretome) composing RAW264.7 conditioned media previously stimulated with anti-Sema4D. The proteomic approach resulted in the identification of more than a thousand proteins

(Supplementary Table 2). Using Gene Set Enrichment Analysis (GSEA) bioinformatics tool, we showed a statistical enrichment in proteins related to important macrophage functions: cell migration, cell projection, cytoskeleton and RAC1 pathway (grouped in migration); DNA replication and cell cycle (grouped in proliferation); FCγR mediated phagocytosis and immunological synapse (grouped in activation) (Supplementary Figure 10). Taken together, the analysis of the secretome by proteomic profiling suggests a direct effect of Sema4D upon macrophage activity, specially affecting their migration, proliferation and activation.

Tumor-associated macrophages are promoting invasion in βTC4 cells as a response to anti-Sema4D treatment

To check the behaviour of TAMs in tumor periphery, the number of macrophages in the perimeter of the base protrusions of invasive fronts was determined after co-staining Sema4D with F4/80 macrophage marker and the RIP1-Tag2 tumor cell marker insulin (Figure 5A). Contrary to the intratumoral results, the number of macrophages in the invasive fronts remained unaltered after anti-Sema4D treatment (Figure 5B). The number of peritumoral Sema4D negative macrophages decreased, while the number of Sema4D positive macrophages and their percentage are strongly increased after treatment (Figure 5D). The abrupt change in macrophage number and phenotype may indicate a role for these cells in the invasive and malignization process that occurs after the therapy.

To confirm this hypothesis, an *in vitro* matrigel invasion assay using βTC4 cells was performed. The addition of conditioned medium of RAW264.7 cell line treated with anti-Sema4D significantly increased the invasive properties of βTC4 cells (Figure 5E). Nevertheless, conditioned media from neither Sema4D, CD72 nor PlxnB2 knockdown RAW264.7 cells did not recapitulate this tumor cell invasion increase (Figure 5F). On the other hand, conditioned media of anti-Sema4D treated shSema4D RAW264.7 cells did not induce an increase, but rather a decrease of tumor cell invasion (Supplementary Figure 11). Therefore, Sema4D retrograde signaling engagement by anti-Sema4D produces a switch of the macrophage phenotype that potentiates tumor cell invasion in RIP1-Tag2, probably by promoting secretion of a pro-invasive molecule.

SDF1/CXCL12 is responsible for promoting invasion as a response to anti-Sema4D treatment

In pursuance of identifying the pro-invasive molecule secreted by macrophages and responsible for tumor cell invasion after anti-Sema4D therapy, a mouse cytokine array was performed in supernatants of RAW264.7 conditioned media. Even though not many significant changes were observed between different treatment conditions (Supplementary table 3), a statistically significant increase in stromal cell-derived factor 1 (SDF1, also known as CXCL12) molecule was detected in anti-Sema4D treated supernatant (Figure 6A). An ELISA analysis of secreted SDF1 revealed an increase in anti-Sema4D condition which was not observed neither in control or treated Sema4D knockdown macrophages (Figure 6B), nor in cells treated with recombinant PlxnB2 (Supplementary Figure 12A) or receptor-knockdown cells (Supplementary Figure 12). We validated SDF1 as a possible macrophage secreted candidate responsible for cancer cell invasion in the RIP1-Tag2 model by an invasion assay in the *in vitro* setting. As expected, βTC4 cells responded to recombinant SDF1 stimulation *in vitro* by

increasing their invasion (Figure 6C). This phenomenon was inhibited when CXCR4 receptor was blocked by its antagonist AMD3100. In addition, the increase observed in βTC4 cells' invasion after anti-Sema4D treated conditioned media addition is comparable to the one produced when exogenous SDF1 was added to IgG1 treated conditioned medium (Figure 6D). Consistently, when AMD3100 was added to anti-Sema4D treated conditioned medium, the invasive capability of βTC4 cells dropped to basal levels, confirming that SDF1 is one of the factors secreted by macrophages after anti-Sema4D treatment responsible for tumor cell invasion.

Finally, we sought to check whether in RIP1-Tag2 model the SDF1/CXCR4 signaling axis was present and affected by anti-Sema4D treatment. We found an increased trend of both CXCR4 and SDF1 RNA expression in treated tumors (Supplementary Figure 12C-D), that was further confirmed by immunohistochemistry (Figure 6E-F). CXCR4 receptor appears to be expressed homogeneusly by RIP1-Tag2 tumor cells, albeit at low levels in control samples and highly present in anti-Sema4D treated mice (Figure 6E), possibly due to an SDF1-induced positive feed-forward mechanism (34). Indeed, CXCR4 is naturally present in the tumor progression stages of RIP1-Tag2 mice, showing expression in metastases, both in control and anti-Sema4D treated mice (Supplementary Figure 12E-F). Therefore, anti-Sema4D treatment seems to exacerbate an already existing CXCR4-mediated metastasis mechanism. As expected, SDF1 was found both in cells with a vascular phenotype and also in round shaped cells compatible with immune infiltrates. The count of the latter showed an increase in SDF1 positive round cells after the treatment (Figure 6F). A costaining of both Sema4D and SDF1 showed an enrichment in SDF1/Sema4D double positive cells after the treatment (Supplementary Figure 12G and Figure 6G). Since endothelial cells also express SDF1, we analyzed the behavior of HUVEC cells in response to anti-Sema4D, observing no changes in gene expression but an increase in SDF1 release after the treatment (Supplementary Figure 13).

Altogether, the *in vivo* results may suggest a tumor-independent origin of SDF1 that could bind to its receptor in RIP1-Tag2 tumor cells to exert its activity. Furthermore, a deeper analysis associating SDF1 levels and invasive capacity of the tumor front revealed a relationship between the invasive capacity and ligand concentration in control tumors (Figure 6H). This relationship was slightly lost after anti-Sema4D treatment.

Clinical relevance of Sema4D and SDF1/CXCR4 axis

After demonstrating both *in vitro* and *in vivo* the role of Sema4D and SDF1/CXCR4 in tumor malignization of the RIP1Tag2 mouse model, we sought to decipher whether these same mechanisms could be also playing the role in the clinical setting. We found Sema4D expression to be significantly increased in metastatic samples when compared to either primary non-malignant and malignant tumors or normal pancreatic controls (Figure 7A). Besides, whereas SDF1 expression remained practically unaltered, we found a significant increase in CXCR4 receptor expression between normal and both primary tumor subtypes and metastases (Figure 7B-C). In fact, there is a gradual increase of CXCR4 that correlates with malignization, thus implying a role for this protein as a tumor progression driver. Furthermore, we evaluated the correlation between Sema4D and CXCR4 expression in non-malignant (non-

metastatic) and malignant (metastatic) primary tumor samples of PanNET patients. Contrary to non-metastatic patients, malignant patients showed higher levels of CXCR4 that showed a correlation with Sema4D (Figure 7D). We finally validated our results using the human macrophage cell line, THP-1 (Figure 7E-F). After anti-Sema4D treatment, THP-1 cells demonstrated an increased migratory phenotype and SDF1 release (Figure 7E-F), without alteration of CXCL12 or CXCR4 expression (Supplementary Figure 14). Overall, the clincal data validates a possible link of SemaD-SDF1/CXCR4 in patient samples of PanNET.

DISCUSSION

Compared to the canonical VEGF, Sema4D is a molecule with quite a different role in angiogenesis since its binding to PlxnB1 can promote different and sometimes opposing cellular responses including vascular guidance (35). Indeed, these differences in vascular targeting potential provide an explanation for the negligible effects in endothelial structures after anti-Sema4D treatment without reduction in MVD and no increased levels of tumor hypoxia. Nevertheless, by PDGF-B reduction anti-Sema4D treatment produced a pericyte structural alteration that functionally modified vessel perfusion and hyperpermeability, thus altering tumor growth.

Moreover, it is widely accepted that a partial inhibition of angiogenesis would not produce an increase of hypoxia within tumours and could not trigger the secondary unwanted pro-invasive and malignant effects (27). Contrarily, we have observed that although anti-Sema4D therapy produced a partial effect in vessel functionality, without induction of hypoxia, it still produced the same pro-invasive effect as anti-VEGF therapy in the PanNET model.

Anti-Sema4D promotes tumor invasion via Tumor-associated macrophages

Protumoral roles for Sema4D typically involve tumor cell-derived Sema4D and there is little evidence about the role of stromal Sema4D (36), Interestingly, in RIP1-Tag2 tumors, the main source of Sema4D are macrophages infiltrating the tumor stroma. In recent years, a critical role for tumor microenvironment and particularly TAMs has been demonstrated (37,38). Their contribution to tumor growth and progression has even been reported in the clinical setting, with correlation between a high intratumor TAM content and a poor prognosis (38). In this study we observe an increase in SEMA4D positive macrophages inside tumors and in the invasive front, which goes in agreement with previously published data where Sema4D controls immune cell motility (10)(39). Our knockdown and recombinant Sema4D experiments strongly suggest that the antibody mediates a Sema4D-dependent retrograde signaling engagement in the membrane of macrophages, rather than a function blocking effect. This retrograde signaling has been previously published for this family of transmembrane proteins in different settings (reviewed in 32 and 33). Furthermore, we validated these results utilizing another anti-Sema4D antibody clone 3B4, but not with clone SK-3, which demonstrates these are antibody-specific effects over macrophages.

SDF1/CXCR4 signaling axis has an important role in cancer progression (40). *In vitro*, we have proven the chemoattractant capacity of SDF1 and its stromal origin, and we have demonstrated that SDF1 release from macrophages is dependent on Sema4D

expression and independent of its receptors. *In vivo*, our results show tumor cells ability to respond to SDF1 stimulus, both in primary tumors and metastases, and the existence of a receptor-ligand positive feedback loop. In fact, the correlation between the invasive capacity of the tumor and SDF1 concentration in control tumors, which is lost after anti-Sema4D treatment, suggests that the SDF1/CXCR4 signaling cascade is already activated regardless of the invasive capacity of the treated tumors.

In the clinical setting, VX15/2503, the humanized anti-Sema4D antibody, showed promising results in the first-in-human phase I clinical trial, with a 45% of patients exhibiting the absence of disease progression for at least 8 weeks (17). Consistently, our own data show anti-Sema4D antibody inhibits tumour growth of PanNETs with a tendency to increase lifespan but also invasion and metastasis. This latter adaptive response to treatment has not been evaluated in patients. Importantly, the combined expression of Sema4D and PlxnB1 is an independent risk factor for disease relapse in colorectal cancer. (41). Other tumors where Sema4D overexpression has been reported as a negative prognostic marker include breast, ovary, soft tissue sarcomas and pancreas (42–44). Our data demonstrate that both Sema4D and CXCR4 expression increase with tumor progression in PanNETs and also a positive correlation between Sema4D and CXCR4 expression in metastatic PanNET samples. Thus implying that Sema4D and CXCR4 expression are related to the malignization process in patients. Taking into account the inexistence of anti-Sema4D treated PanNET patient samples, these study remarks the role of Sema4D as a potential candidate of tumor malignization in this type of tumors. We have proven, using *in vitro*, *in vivo* and *in silico* approaches, that stromal or immune cells are the primary source of Sema4D, rather than tumor cells.

In conclusion, we describe a hypoxia independent novel mechanism of tumor malignization in the RIP1-Tag2 model, where the signaling engagement of anti-Sema4D antibody binding to Sema4D in macrophages seems to be responsible for the malignant phenotype via SDF1/CXCR4 signaling axis activation (Figure 7G). Our study suggests a combinantion of anti-Sema4D therapy and small molecule inhibitors of selected macrophage functions coud be a new therapeutical strategy for PanNET patients. Future studies combining non-traditional anti-angiogenics and novel immunotherapies would undoubtedly shed light into the role of tumor-associated cells, allowing overcoming the undesired resistance.

ACKNOWLEDGEMENTS

The authors would like to thank Vaccinex Inc. for providing reagents and research money (<20.000 Eur) to support this work, especially to Maurice Zauderer, Ernest S. Smith and Elizabeth E. Evans for their critical discussions and helpful suggestions in the manuscript. We are also very thankful to Alba López for expert technical support with the animal colony and Álvaro Aytés for critical reading of the manuscript and helpful suggestions.

REFERENCES

1. Fraisl P, Mazzone M, Schmidt T, Carmeliet P. Regulation of Angiogenesis by Oxygen and Metabolism. Dev Cell [Internet]. 2009 [cited 2017 Dec 25];16:167–79. Available from: http://www.ncbi.nlm.nih.gov/pubmed/19217420
2. Pennacchietti S, Michieli P, Galluzzo M, Mazzone M, Giordano S, Comoglio PM. Hypoxia promotes invasive growth by transcriptional activation of the met protooncogene. Cancer Cell. 2003;3:347–61.
3. Schindl M, Schoppmann SF, Samonigg H, Hausmaninger H, Kwasny W, Gnant M, et al. Overexpression of hypoxia-inducible factor 1alpha is associated with an unfavorable prognosis in lymph node-positive breast cancer. Clin Cancer Res. 2002;8:1831–7.
4. Semenza GL. HIF-1 and tumor progression: pathophysiology and therapeutics. Trends Mol Med. 2002;8:S62-7.
5. Zhong H, De Marzo AM, Laughner E, Lim M, Hilton DA, Zagzag D, et al. Overexpression of hypoxia-inducible factor 1alpha in common human cancers and their metastases. Cancer Res. 1999;59:5830–5.
6. Worzfeld T, Offermanns S. Semaphorins and plexins as therapeutic targets. Nat Rev Drug Discov [Internet]. 2014 [cited 2017 Dec 25];13:603–21. Available from: http://www.ncbi.nlm.nih.gov/pubmed/25082288
7. Kolodkin AL, Matthes DJ, Goodman CS. The semaphorin genes encode a family of transmembrane and secreted growth cone guidance molecules. Cell. 1993;75:1389–99.
8. Kruger RP, Aurandt J, Guan K-L. Semaphorins command cells to move. Nat Rev Mol Cell Biol [Internet]. 2005 [cited 2017 Dec 25];6:789–800. Available from: http://www.nature.com/doifinder/10.1038/nrm1740
9. Tamagnone L, Comoglio PM. Signalling by semaphorin receptors: cell guidance and beyond. Trends Cell Biol [Internet]. 2000 [cited 2017 Dec 25];10:377–83. Available from: http://www.ncbi.nlm.nih.gov/pubmed/10932095
10. Delaire S, Billard C, Tordjman R, Chédotal A, Elhabazi A, Bensussan A, et al. Biological activity of soluble CD100. II. Soluble CD100, similarly to H-SemaIII, inhibits immune cell migration. J Immunol. 2001;166:4348–54.
11. Kumanogoh A, Watanabe C, Lee I, Wang X, Shi W, Araki H, et al. Identification of CD72 as a lymphocyte receptor for the class IV semaphorin CD100: a novel mechanism for regulating B cell signaling. Immunity. 2000;13:621–31.
12. Basile JR, Castilho RM, Williams VP, Gutkind JS. Semaphorin 4D provides a link between axon guidance processes and tumor-induced angiogenesis. Proc Natl Acad Sci U S A [Internet]. 2006 [cited 2017 Dec 19];103:9017–22. Available from: http://www.pnas.org/cgi/doi/10.1073/pnas.0508825103
13. Dirkx AEM, Oude Egbrink MGA, Wagstaff J, Griffioen AW. Monocyte/macrophage infiltration in tumors: modulators of angiogenesis. J Leukoc Biol [Internet]. 2006 [cited 2017 Dec 19];80:1183–96. Available from: http://www.jleukbio.org/cgi/doi/10.1189/jlb.0905495
14. Sierra JR, Corso S, Caione L, Cepero V, Conrotto P, Cignetti A, et al. Tumor angiogenesis and progression are enhanced by Sema4D produced by tumor-associated macrophages. J Exp Med [Internet]. 2008 [cited 2017 Dec 25];205:1673–85. Available from: http://www.ncbi.nlm.nih.gov/pubmed/18559453
15. Basile JR, Holmbeck K, Bugge TH, Gutkind JS. MT1-MMP controls tumor-induced angiogenesis through the release of semaphorin 4D. J Biol Chem [Internet]. 2007 [cited 2017 Dec 19];282:6899–905. Available from: http://www.jbc.org/lookup/doi/10.1074/jbc.M609570200
16. Elhabazi A, Delaire S, Bensussan A, Boumsell L, Bismuth G. Biological activity of soluble CD100. I. The extracellular region of CD100 is released from the surface of T lymphocytes by regulated proteolysis. J Immunol. 2001;166:4341–7.
17. Patnaik A, Weiss GJ, Leonard JE, Rasco DW, Sachdev JC, Fisher TL, et al. Safety, Pharmacokinetics, and Pharmacodynamics of a Humanized Anti-Semaphorin 4D Antibody, in a First-In-Human Study of Patients with Advanced

Solid Tumors. Clin Cancer Res [Internet]. 2016 [cited 2018 Jul 24];22:827–36. Available from: http://www.ncbi.nlm.nih.gov/pubmed/26446947
18. Hanahan D. Heritable formation of pancreatic beta-cell tumours in transgenic mice expressing recombinant insulin/simian virus 40 oncogenes. Nature. 1985;315:115–22.
19. Pàez-Ribes M, Allen E, Hudock J, Takeda T, Okuyama H, Viñals F, et al. Antiangiogenic therapy elicits malignant progression of tumors to increased local invasion and distant metastasis. Cancer Cell [Internet]. 2009 [cited 2017 Dec 19];15:220–31. Available from: http://linkinghub.elsevier.com/retrieve/pii/S1535610809000348
20. Fisher TL, Reilly CA, Winter LA, Pandina T, Jonason A, Scrivens M, et al. Generation and preclinical characterization of an antibody specific for SEMA4D. MAbs [Internet]. Taylor & Francis; 2016 [cited 2018 Jul 24];8:150–62. Available from: http://www.ncbi.nlm.nih.gov/pubmed/26431358
21. Casanovas O, Hicklin DJ, Bergers G, Hanahan D. Drug resistance by evasion of antiangiogenic targeting of VEGF signaling in late-stage pancreatic islet tumors. Cancer Cell [Internet]. 2005 [cited 2017 Dec 19];8:299–309. Available from: http://linkinghub.elsevier.com/retrieve/pii/S1535610805002989
22. Missiaglia E, Dalai I, Barbi S, Beghelli S, Falconi M, della Peruta M, et al. Pancreatic endocrine tumors: expression profiling evidences a role for AKT-mTOR pathway. J Clin Oncol [Internet]. 2009/11/18. 2009 [cited 2018 Mar 5];28:245–55. Available from: http://www.ncbi.nlm.nih.gov/pubmed/19917848
23. Sadanandam A, Wullschleger S, Lyssiotis CA, Grotzinger C, Barbi S, Bersani S, et al. A Cross-Species Analysis in Pancreatic Neuroendocrine Tumors Reveals Molecular Subtypes with Distinctive Clinical, Metastatic, Developmental, and Metabolic Characteristics. Cancer Discov [Internet]. 2015 [cited 2018 Mar 5];5:1296–313. Available from: http://www.ncbi.nlm.nih.gov/pubmed/26446169
24. Zhou H, Yang Y-H, Basile JR. The Semaphorin 4D-Plexin-B1-RhoA signaling axis recruits pericytes and regulates vascular permeability through endothelial production of PDGF-B and ANGPTL4. Angiogenesis [Internet]. 2014 [cited 2017 Dec 25];17:261–74. Available from: http://link.springer.com/10.1007/s10456-013-9395-0
25. Ebos JML, Lee CR, Cruz-Munoz W, Bjarnason GA, Christensen JG, Kerbel RS. Accelerated metastasis after short-term treatment with a potent inhibitor of tumor angiogenesis. Cancer Cell [Internet]. 2009 [cited 2017 Dec 25];15:232–9. Available from: http://linkinghub.elsevier.com/retrieve/pii/S1535610809000294
26. Sennino B, Ishiguro-Oonuma T, Wei Y, Naylor RM, Williamson CW, Bhagwandin V, et al. Suppression of tumor invasion and metastasis by concurrent inhibition of c-Met and VEGF signaling in pancreatic neuroendocrine tumors. Cancer Discov [Internet]. American Association for Cancer Research; 2012 [cited 2018 Jul 18];2:270–87. Available from: http://www.ncbi.nlm.nih.gov/pubmed/22585997
27. You W-K, Sennino B, Williamson CW, Falcón B, Hashizume H, Yao L-C, et al. VEGF and c-Met blockade amplify angiogenesis inhibition in pancreatic islet cancer. Cancer Res [Internet]. 2011 [cited 2017 Dec 25];71:4758–68. Available from: http://cancerres.aacrjournals.org/cgi/doi/10.1158/0008-5472.CAN-10-2527
28. Bougeret C, Mansur IG, Dastot H, Schmid M, Mahouy G, Bensussan A, et al. Increased surface expression of a newly identified 150-kDa dimer early after human T lymphocyte activation. J Immunol. 1992;148:318–23.
29. Boumsell L, Schmid M, Dastot H, Gouttefangeas C, Mathieu-Mahul D, Bensussan A. In vitro differentiation from a pluripotent human CD4+CD8+ thymic cloned cell into four phenotypically distinct subsets. J Immunol [Internet]. 1990 [cited 2018 Jun 5];145:2797–802. Available from: http://www.ncbi.nlm.nih.gov/pubmed/1976704
30. Delaire S, Elhabazi A, Bensussan A, Boumsell L. CD100 is a leukocyte semaphorin. Cell Mol Life Sci [Internet]. 1998 [cited 2018 Jun 5];54:1265–76.

Available from: http://link.springer.com/10.1007/s000180050252
31. Hall KT, Boumsell L, Schultze JL, Boussiotis VA, Dorfman DM, Cardoso AA, et al. Human CD100, a novel leukocyte semaphorin that promotes B-cell aggregation and differentiation. Proc Natl Acad Sci U S A [Internet]. 1996 [cited 2018 Jun 5];93:11780–5. Available from: http://www.ncbi.nlm.nih.gov/pubmed/8876214
32. Jongbloets BC, Pasterkamp RJ. Semaphorin signalling during development. Development [Internet]. Oxford University Press for The Company of Biologists Limited; 2014 [cited 2019 Apr 1];141:3292–7. Available from: http://dev.biologists.org/content/141/17/3292
33. Zhou Y, Gunput RA, Pasterkamp RJ. Semaphorin signaling: progress made and promises ahead. Trends Biochem Sci [Internet]. 2008/04/01. 2008;33:161–70. Available from: http://www.ncbi.nlm.nih.gov/entrez/query.fcgi?cmd=Retrieve&db=PubMed&dopt=Citation&list_uids=18374575
34. Shibata W, Ariyama H, Westphalen CB, Worthley DL, Muthupalani S, Asfaha S, et al. Stromal cell-derived factor-1 overexpression induces gastric dysplasia through expansion of stromal myofibroblasts and epithelial progenitors. Gut. 2013 Feb;62(2):192-200. doi: 10.1136/gutjnl-2011-301824. PMID: 22362916
35. Giordano S, Corso S, Conrotto P, Artigiani S, Gilestro G, Barberis D, et al. The semaphorin 4D receptor controls invasive growth by coupling with Met. Nat Cell Biol [Internet]. 2002 [cited 2017 Dec 25];4:720–4. Available from: http://www.nature.com/articles/ncb843
36. Ch'ng ES, Kumanogoh A. Roles of Sema4D and Plexin-B1 in tumor progression. Mol Cancer [Internet]. 2010 [cited 2018 Mar 5];9:251. Available from: http://molecular-cancer.biomedcentral.com/articles/10.1186/1476-4598-9-251
37. Albini A, Sporn MB. The tumour microenvironment as a target for chemoprevention. Nat Rev Cancer [Internet]. 2007 [cited 2018 Mar 5];7:139–47. Available from: http://www.ncbi.nlm.nih.gov/pubmed/17218951
38. Balkwill F, Mantovani A. Inflammation and cancer: back to Virchow? Lancet (London, England) [Internet]. 2001 [cited 2018 Mar 5];357:539–45. Available from: http://linkinghub.elsevier.com/retrieve/pii/S0140673600040460
39. Evans EE, Jonason AS, Bussler H, Torno S, Veeraraghavan J, Reilly C, et al. Antibody Blockade of Semaphorin 4D Promotes Immune Infiltration into Tumor and Enhances Response to Other Immunomodulatory Therapies. Cancer Immunol Res [Internet]. 2015 [cited 2017 Dec 25];3:689–701. Available from: http://cancerimmunolres.aacrjournals.org/cgi/doi/10.1158/2326-6066.CIR-14-0171
40. Duda DG, Kozin S V, Kirkpatrick ND, Xu L, Fukumura D, Jain RK. CXCL12 (SDF1alpha)-CXCR4/CXCR7 pathway inhibition: an emerging sensitizer for anticancer therapies? Clin Cancer Res [Internet]. 2011 [cited 2017 Dec 25];17:2074–80. Available from: http://clincancerres.aacrjournals.org/cgi/doi/10.1158/1078-0432.CCR-10-2636
41. Ikeya T, Maeda K, Nagahara H, Shibutani M, Iseki Y, Hirakawa K. The combined expression of Semaphorin4D and PlexinB1 predicts disease recurrence in colorectal cancer. BMC Cancer [Internet]. 2016 [cited 2018 Mar 5];16:525. Available from: http://www.ncbi.nlm.nih.gov/pubmed/27456345
42. Valente G, Nicotra G, Arrondini M, Castino R, Capparuccia L, Prat M, et al. Co-expression of plexin-B1 and Met in human breast and ovary tumours enhances the risk of progression. Cell Oncol [Internet]. 2009 [cited 2017 Dec 25];31:423–36. Available from: http://www.ncbi.nlm.nih.gov/pubmed/19940359
43. Campos M, De Campos SGP, Ribeiro GG, Eguchi FC, Da Silva SRM, De Oliveira CZ, et al. Ki-67 and CD100 immunohistochemical expression is associated with local recurrence and poor prognosis in soft tissue sarcomas, respectively. Oncol Lett [Internet]. 2013 [cited 2018 Sep 18];5:1527–35.

Available from: http://www.ncbi.nlm.nih.gov/pubmed/23759874
44. Kato S, Kubota K, Shimamura T, Shinohara Y, Kobayashi N, Watanabe S, et al. Semaphorin 4D, a lymphocyte semaphorin, enhances tumor cell motility through binding its receptor, plexinB1, in pancreatic cancer. Cancer Sci [Internet]. 2011 [cited 2018 Jul 27];102:2029–37. Available from: http://www.ncbi.nlm.nih.gov/pubmed/21812859

FIGURE LEGENDS

Figure 1. Anti-Sema4D treatment demonstrates anti-tumor effects and extends survival by vascular targeting. A) Quantification of tumor volume of untreated (Ctrl), anti-Sema4D (α-S4D) and anti-VEGFR2 (α-VR2) treated for 4 wks (n≥10). **B)** Kaplan-Meier survival curves. Log rank test 0.0027 (n≥20). **C,E)** Quantification of the number of vessel structures (MVD) by CD31 staining and the CD31 area density (%) per field of viable tumor. **D,F,G)** The percentage of the area of type IV collagen, vascular cadherin (VE-cadherin) or the vascular structures covered by different pericyte markers (Desmin, NG2 and α-SMA) per field of viable tumor normalized by the total number of vessel structures. **H)** Quantification of the percentatge of tumors with vessel microhemorraging. **C-H.** All treatments were performed during 4 weeks. Mann-Whitney test (n≥10 except for pericyte coverage, n≥5).

Figure 2. Therapy-induced local invasiveness and distant metastasis. A) H&E staining of tumors of untreated (ctrl), anti-Sema4D (α-S4D) and anti-VEGFR2 (α-VR2) treated animals for 2 wks. **B)** Quantification of tumor invasiveness of encapsulated, microinvasive and highly invasive tumors per animal after short (2 wks, left) and long (4 wks, right) treatment with anti-Sema4D and anti-VEGFR2. Fisher exact probability test (n≥5). **C left)** Enlarged lymph node after 4-weeks anti-Sema4D treatment (first picture). The presence of tumor cells inside the lymph node is corroborated with T antigen staining (second picture). **C right)** H&E of micrometastasis in liver after 4-weeks anti-Sema4D therapy (third picture) and its respective T antigen staining corroboration (forth picture). **D**) Incidence of lymph node metastasis (left) and liver micrometastasis (right) after the anti-Sema4D or the anti-VEGFR2 treatment for 4 weeks compared to untreated control animals. Chi-square test (n≥10). **E)** Quantification of the number of liver metastatic lesions in control, anti-Sema4D and anti-VEGFR2 treated animals after 4 weeks of treatment. Mann-Whitney test (n=4).

Figure 3. Anti-Sema4D treatment-related malignization does not produce intratumor hypoxia and neither alters c-Met expression nor its activation. A) Immunohistochemistry staining for Glut1 and pimonidazole (pimo) in untreated (ctrl), anti-Sema4D (α-S4D) and anti-VEGFR2 (α-V2R) treated samples. **B)** Quantification of the incidence of hypoxic tumors after anti-Sema4D and anti-VEGFR2 1 week treatment compared to controls by staining of pimonidazole adducts (n≥132). **C)** Quantification by Glut1 staining of the incidence of hypoxic tumors in anti-Sema4D and anti-VEGFR2 2 wks short-term (left) and 4 wks long-term (right) treatments compared to controls (n≥75). **B-C.** Mann-Whitney test. **D)** qRT-PCR Taqman analysis of *c-met* relative to *Hprt1* housekeeping gene expression. RNA from RIP1-Tag2 untreated or anti-Sema4D treated mice was analyzed. Mann-Whitney test (n=3). **E)** Western blot analysis of the active form of c-Met protein (phospho c-met) in control and α-S4D treated RIP1-Tag2

tumors. α-tubulin protein is used as a housekeeping control. Lysate from A549 cells treated with HGF in equal conditions was used as a positive control for c-met phosphorylation. RAW cell line was used as a negative control. **F)** qRT-PCR Taqman analysis of *c-met* relative to *Hprt1* housekeeping gene expression. RNA from βTC4 cells was analysed and RNA from murine kidney tissue was used as a positive control. **G)** Western blot analysis of the active form of c-Met protein (phospho c-met) in two independent samples of control, anti-Sema4D (α-S4D) and HGF treated βTC4 cells. α-tubulin protein is used as a housekeeping control. Lysate from A549 cells treated with HGF in equal conditions was used as a positive control for c-met phosphorylation. RAW cell line was used as a negative control.

Figure 4. Tumor-associated macrophages respond to anti-Sema4D treatment increasing their migration. A) Double immunofluorescence of Sema4D and F4/80 in IgG1 and anti-Sema4D (α-S4D) treated samples (2 wks treatment). White arrows reveal the expression of Sema4D by some TAMs. **B-D)** Quantification of the number of intratumoral total TAMs, Sema4D negative TAMs or Sema4D positive TAMs per field and the percentage of intratumoral Sema4D positive TAMs per total number of TAMs. IgG1 treated mice were used as a control. Mann-Whitney test (n≥20). **E)** Quantification of the number of migrated RAW 264 cells per field in untreated, IgG1, anti-Sema4D and recombinant Sema4D (rS4D) treatment conditions. Results are presented as number of migrated cells per field normalized by the untreated control. Mann-Whitney test (n≥45). **F)** Quantification of the number of migrated RAW 264 cells per field in parental and sh Sema4D, sh CD72, sh PlexinB2 and sh NS RAW 264 cells. Results are presented as number of migrated cells per field normalized by the parental control. Mann-Whitney test (n≥30). **G)** Quantification of the number of migrated RAW 264 cells per field in untreated and anti-Sema4D treatment conditions in sh Sema4D ans sh NS (non-silencing control) RAW 264 cells. Mann-Whitney test (n≥45).

Figure 5. Increase in the number of peritumoral Sema4D positive macrophages in the tumor invasive fronts and response to anti-Sema4D therapy by increasing βTC4 invasion potential. A) Triple immunofluorescence co-staining for Insulin, F4/80 and Sema4D in tumor fronts of IgG1 and anti-Sema4D treated animals. **B-D)** Quantification of the number of peritumoral total TAMs, Sema4D negative TAMs or Sema4D positive TAMS normalized by the perimeter of the base tumor protrusions (μm) in the invasive fronts and the percentage of Sema4D positive TAMs per total of TAMs. Mann-Whitney test (n≥20). IgG1 treated mice were used as a control. **E)** Quantification of invasive βTC4 cells per field in the presence of the conditioned media of untreated, IgG1 added or treated and anti-Sema4D added or treated RAW 264 cells used as chemoattractant in Matrigel® transwell assay. IgG1 treatment is used as an isotype control. Results are presented as number of invasive cells per field normalized by the untreated control. Representative experiment of n=3. Mann-Whitney test (n>19 fields). **F)** Quantification of invasive βTC4 cells per field in the presence of the conditioned media of parental, sh Sema4D, sh CD72, sh PlexinB2 and sh NS (non-silencing control) RAW 264 cells used as chemoattractant in Matrigel® transwell assay. Results are presented as number of invasive cells per field normalized by the parental control. Representative experiment of n=3. Mann-Whitney test (n>20 fields).

Figure 6. SDF1/CXCR4 axis is responsible for promoting invasion after anti-Sema4D treatment and is present *in vivo*. A) Levels of stromal cell-derived factor 1 (SDF1) in supernatants of RAW 264 cells treated with IgG1 or anti-Sema4D. Anti-Sema4D added medium was used as a control. T-test (n=4). **B)** Quantification of SDF1 protein release by ELISA analysis of conditioned media from control and anti-Sema4D treated RAW parental and sh Sema4D cells. Results are presented as ng of SDF1 per total protein µg for each condition normalized by the untreated controls. Mann-Whitney test (n=3). **C)** Quantification of *in vitro* matrigel invasion assay of βTC4 cells in presence of basal medium, medium containing SDF1, AMD3100 or both. Results are presented as number of invasive cells per field normalized by the basal control. Representative experiment of n=3. Mann-Whitney test (n≥ 30 fields). **D)** Quantification of *in vitro* matrigel invasion assay in which βTC4 cells were incubated with conditioned media from RAW 264 cells untreated or treated with IgG1 or anti-Sema4D in presence of SDF1 or its AMD3100. Results are presented as number of invasive cells per field normalized by the untreated control. Representative experiment of n=3. Mann-Whitney test (n≥ 30 fields). **E)** Immunohistochemistry (left) and quantification (right) of the incidence of CXR4 expressing tumors in control and anti-Sema4D treated mice. Chi-square test (n>17 tumors). **F)** Immunohistochemistry (left) and quantification (right) of the number of SDF1 positive round intratumoral cells per field in control and anti-Sema4D treated mice. Mann-Whitney test (n>85 tumors). **G)** Incidence of SDF1 expressing tumors according to the invasive capacity of the tumor fronts and the treatment regime. **H)** Quantification of the number of SDF1 positive Sema4D positive cells per total number of Sema4D positive cells per tumor field of control and anti-Sema4D treated mice. Mann-Whitney test (n>17 tumors).

Figure 7. Clinical validation of the Sema4D-CXCR4 signaling axis. Gene expression analysis of **A)** *SEMA4D*, **B)** *SDF1* and **C)** *CXCR4* genes in normal pancreas islet, non-malignant and malignant primary tumor and their derived metastases from a clinical set of PanNET patients samples (GSE73338). Mann-Whitney test (n≥7). **D)** Correlation analysis of CXCR4 and Sema4D gene expression in non-malignant and malignant primary tumors from a clinical set of PanNET patients samples (GSE73338). Spearman's correlation p (n≥26). **E)** Quantification of the number of migrated THP-1 human macrophage cells per field in untreated and anti-Sema4D treatment conditions. Results are presented as number of migratory cells per field normalized by the untreated control. Mann-Whitney test (n≥30). **F)** Quantification of SDF1 protein release by ELISA analysis of conditioned media from control and anti-Sema4D treated THP-1 cells. Results are presented as ng of SDF1 per total protein µg for each condition normalized by the untreated control. Mann-Whitney test (n=3). **G) Proposed model for anti-Sema4D derived malignization.** Targeting of macrophage derived Sema4D produces macrophage activation and secretion of pro-invasive molecules such as SDF1. Secreted SDF1 is latter bound to its CXCR4 receptor in tumor cells to drive tumor cell invasion. Figure was created using Servier Medical Art according to a Creative Commons Attribution 3.0 Unported License guidelines 3.0 (https://creativecommons.org/licenses/by/3.0/). Simplification and color changes were made to the original cartoons.

Figure 1

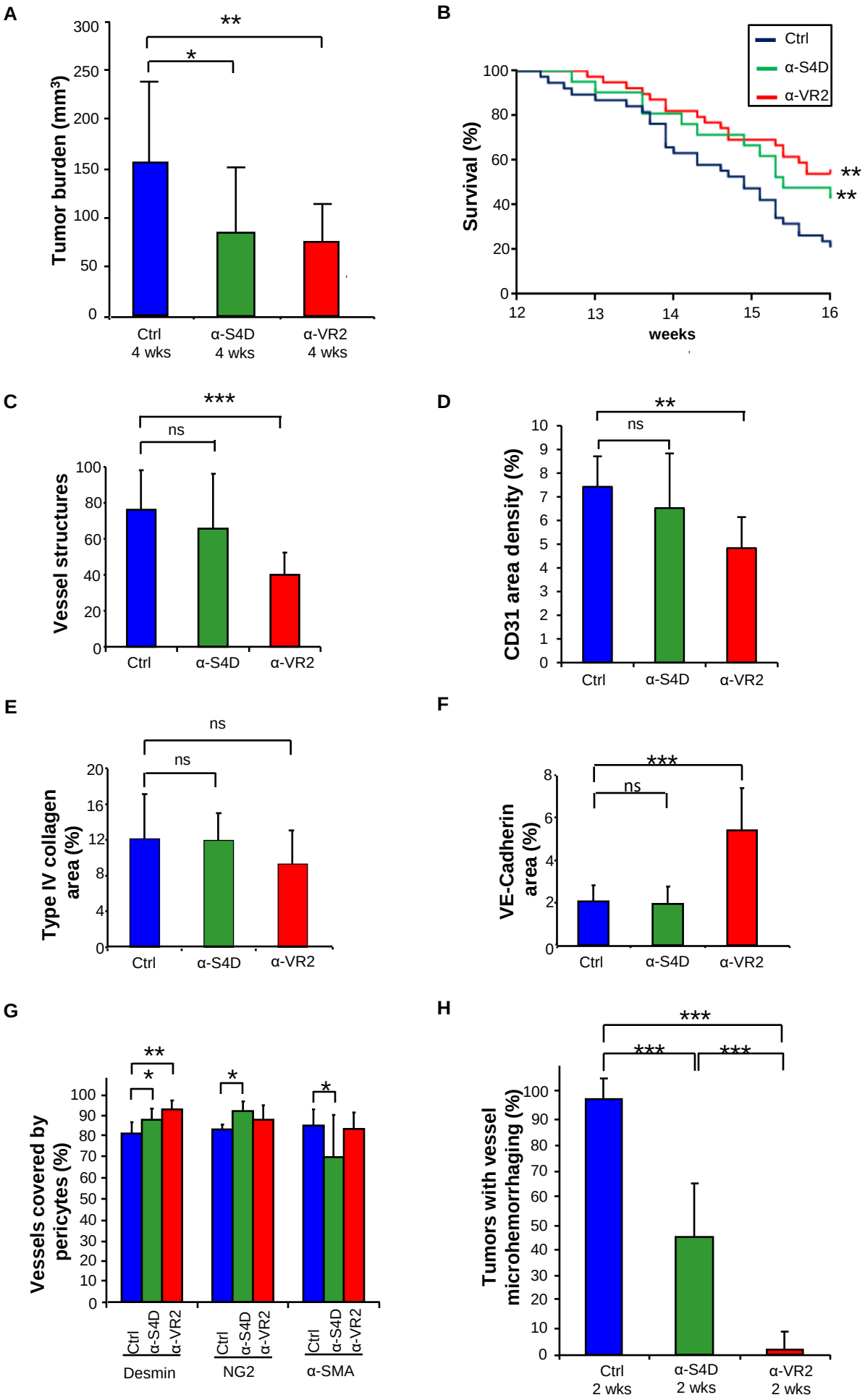
A
Tumor burden (mm³)
300
250
200
150
100
50
0
**
*
Ctrl 4 wks
α-S4D 4 wks
α-VR2 4 wks
B
Survival (%)
100
80
60
40
20
0
12
13
14
15
16
weeks
Ctrl
α-S4D
α-VR2
**
**
C
Vessel structures
***
ns
100
80
60
40
20
0
Ctrl
α-S4D
α-VR2
D
CD31 area density (%)
**
ns
10
9
8
7
6
5
4
3
2
1
0
Ctrl
α-S4D
α-VR2
E
Type IV collagen area (%)
ns
ns
20
16
12
8
4
0
Ctrl
α-S4D
α-VR2
F
VE-Cadherin area (%)
***
ns
8
6
4
2
0
Ctrl
α-S4D
α-VR2
G
Vessels covered by pericytes (%)
**
*
*
*
100
90
80
70
60
50
40
30
20
10
0
Ctrl
α-S4D
α-VR2
Desmin
NG2
α-SMA
H
Tumors with vessel microhemorrhaging (%)
***
***
***
100
90
80
70
60
50
40
30
20
10
0
Ctrl 2 wks
α-S4D 2 wks
α-VR2 2 wks

Figure 2

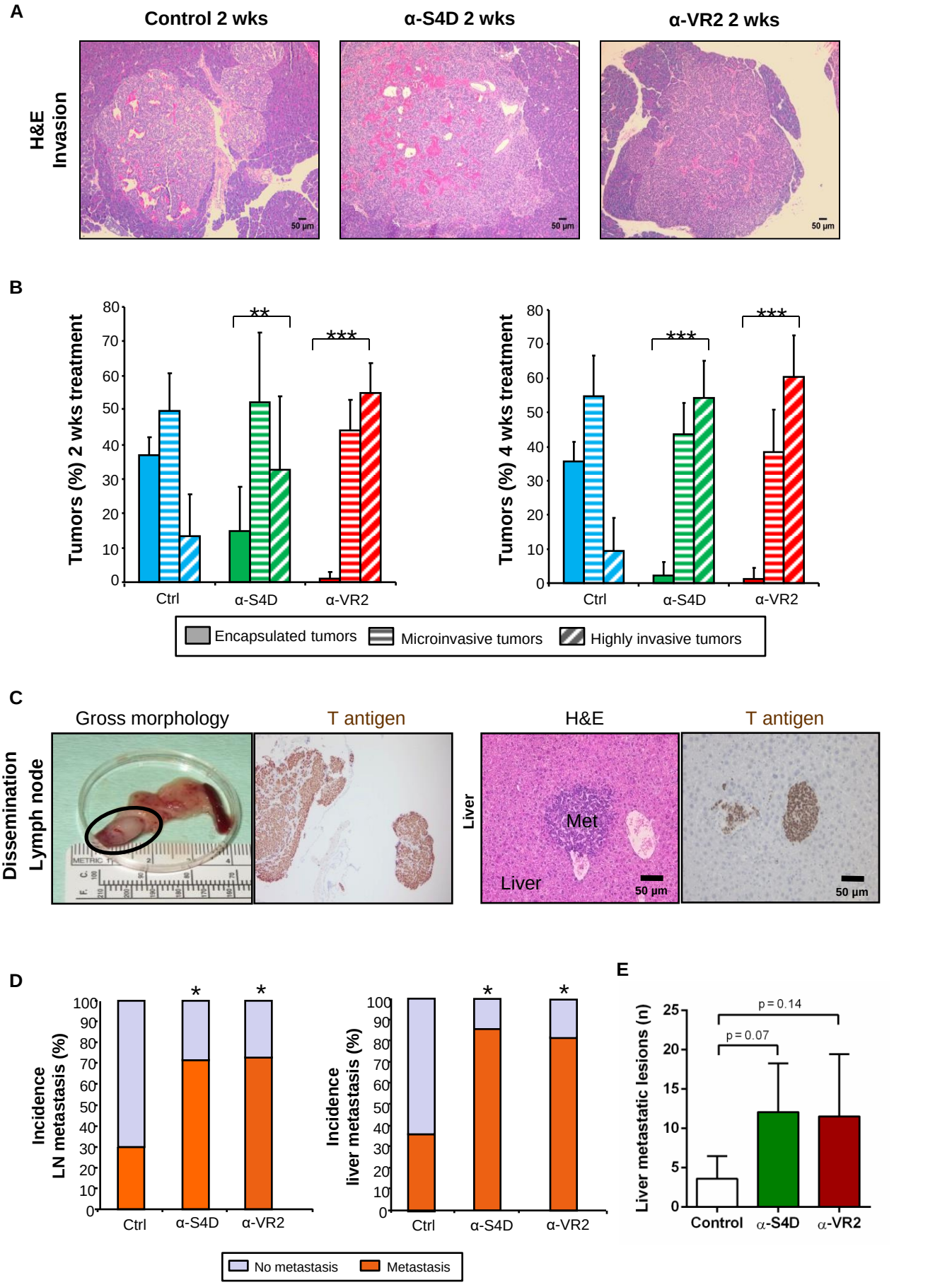
A
Control 2 wks
α-S4D 2 wks
α-VR2 2 wks
H&E Invasion
50 µm
B
Tumors (%) 2 wks treatment
Tumors (%) 4 wks treatment
**
***
Ctrl
α-S4D
α-VR2
Encapsulated tumors
Microinvasive tumors
Highly invasive tumors
C
Gross morphology
T antigen
H&E
Dissemination Lymph node
Liver
Met
Liver
50 µm
D
Incidence LN metastasis (%)
Incidence liver metastasis (%)
No metastasis
Metastasis
E
Liver metastatic lesions (n)
p = 0.14
p = 0.07
Control
α-S4D
α-VR2

Figure 3

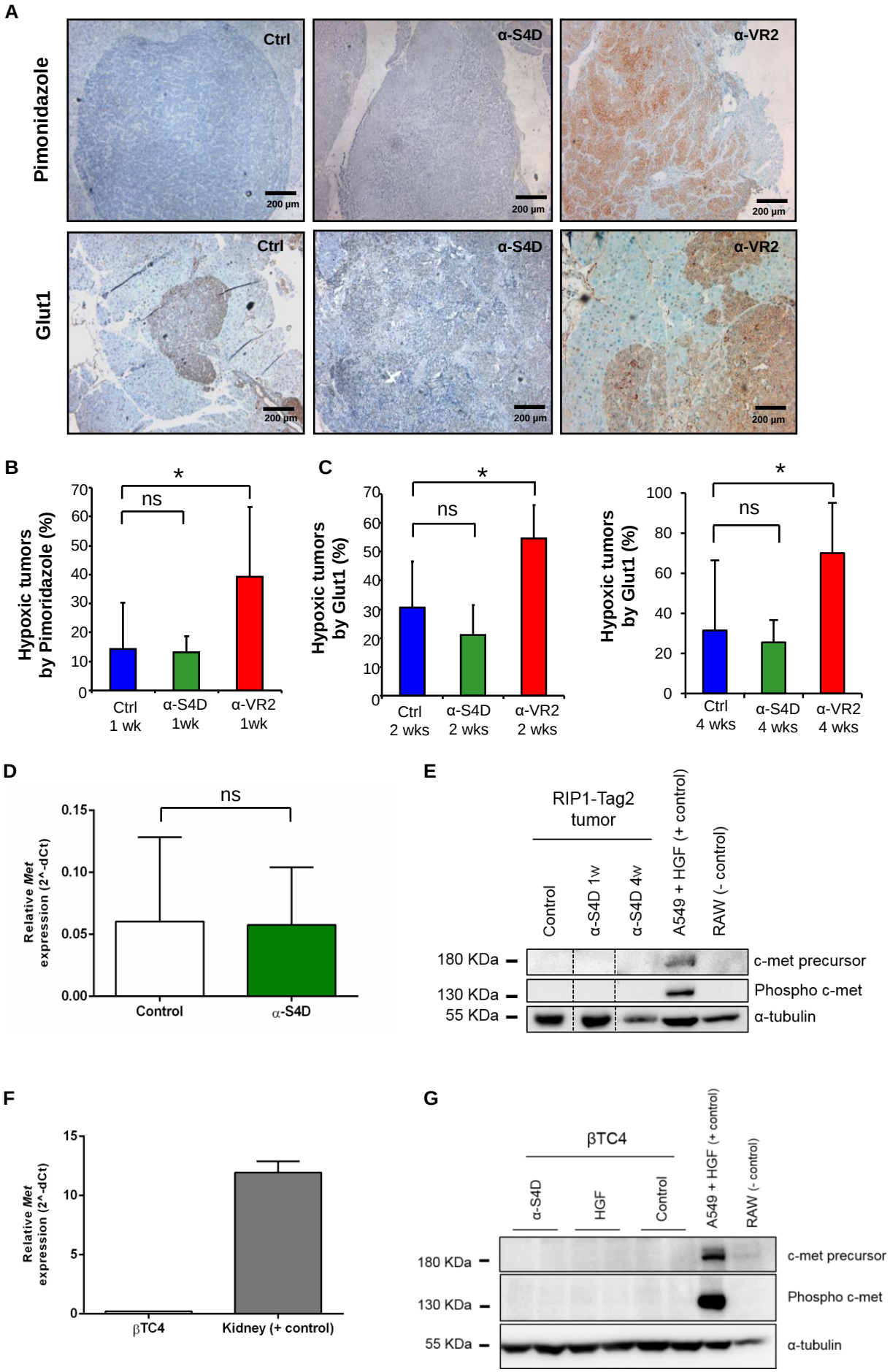
A
Pimonidazole
Glut1
Ctrl
α-S4D
α-VR2
200 µm
B
Hypoxic tumors by Pimoridazole (%)
ns
*
Ctrl 1 wk
α-S4D 1wk
α-VR2 1wk
C
Hypoxic tumors by Glut1 (%)
Ctrl 2 wks
α-S4D 2 wks
α-VR2 2 wks
Ctrl 4 wks
α-S4D 4 wks
α-VR2 4 wks
D
Relative Met expression (2^-dCt)
Control
α-S4D
E
RIP1-Tag2 tumor
Control
α-S4D 1w
α-S4D 4w
A549 + HGF (+ control)
RAW (- control)
180 KDa
130 KDa
55 KDa
c-met precursor
Phospho c-met
α-tubulin
F
βTC4
Kidney (+ control)
G
βTC4
α-S4D
HGF
Control

Figure 4

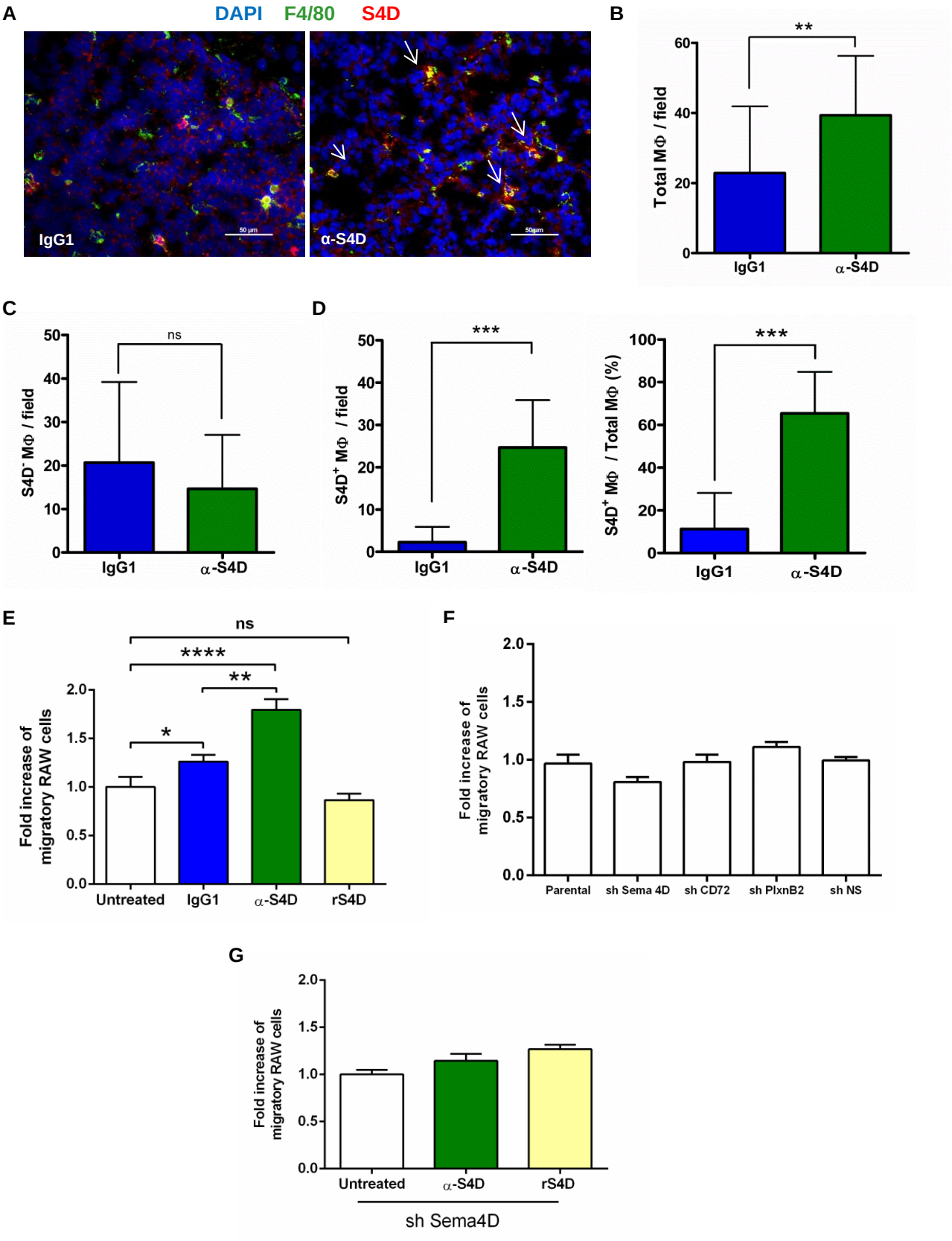
A
DAPI F4/80 S4D
IgG1
α-S4D
B
Total MΦ / field
IgG1
α-S4D
C
S4D- MΦ / field
ns
IgG1
α-S4D
D
S4D+ MΦ / field
S4D+ MΦ / Total MΦ (%)
***
IgG1
α-S4D
E
Fold increase of migratory RAW cells
ns
****
**
*
Untreated
IgG1
α-S4D
rS4D
F
Fold increase of migratory RAW cells
Parental
sh Sema 4D
sh CD72
sh PlxnB2
sh NS
G
Fold increase of migratory RAW cells
Untreated
α-S4D
rS4D
sh Sema4D

Figure 5

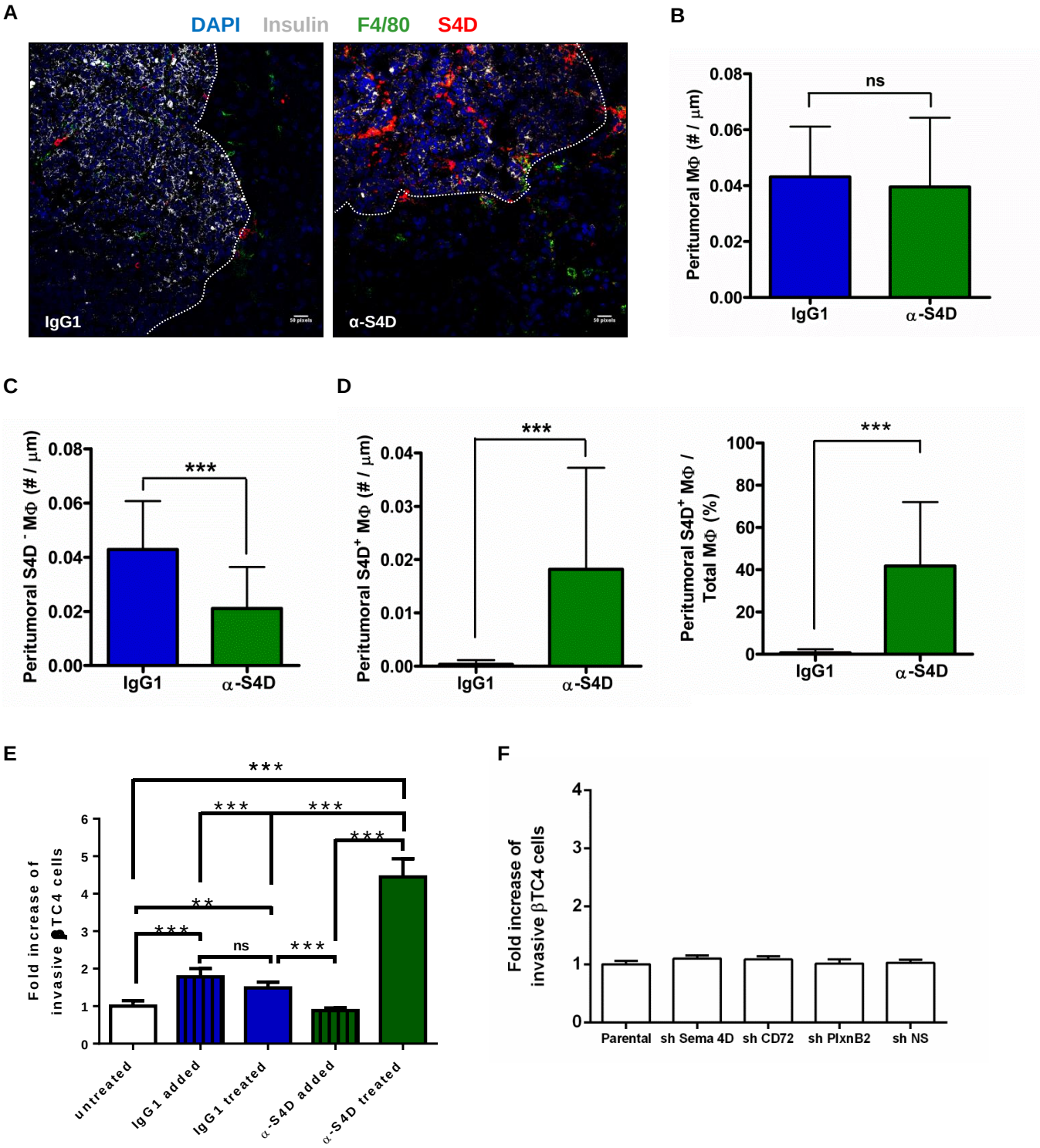
A
DAPI Insulin F4/80 S4D
IgG1
α-S4D
B
Peritumoral MΦ (# / μm)
ns
IgG1
α-S4D
C
Peritumoral S4D⁻ MΦ (# / μm)
***
IgG1
α-S4D
D
Peritumoral S4D⁺ MΦ (# / μm)
***
Peritumoral S4D⁺ MΦ / Total MΦ (%)
***
E
Fold increase of invasive βTC4 cells
***
**
ns
untreated
IgG1 added
IgG1 treated
α-S4D added
α-S4D treated
F
Fold increase of invasive βTC4 cells
Parental
sh Sema 4D
sh CD72
sh PlxnB2
sh NS

Figure 6

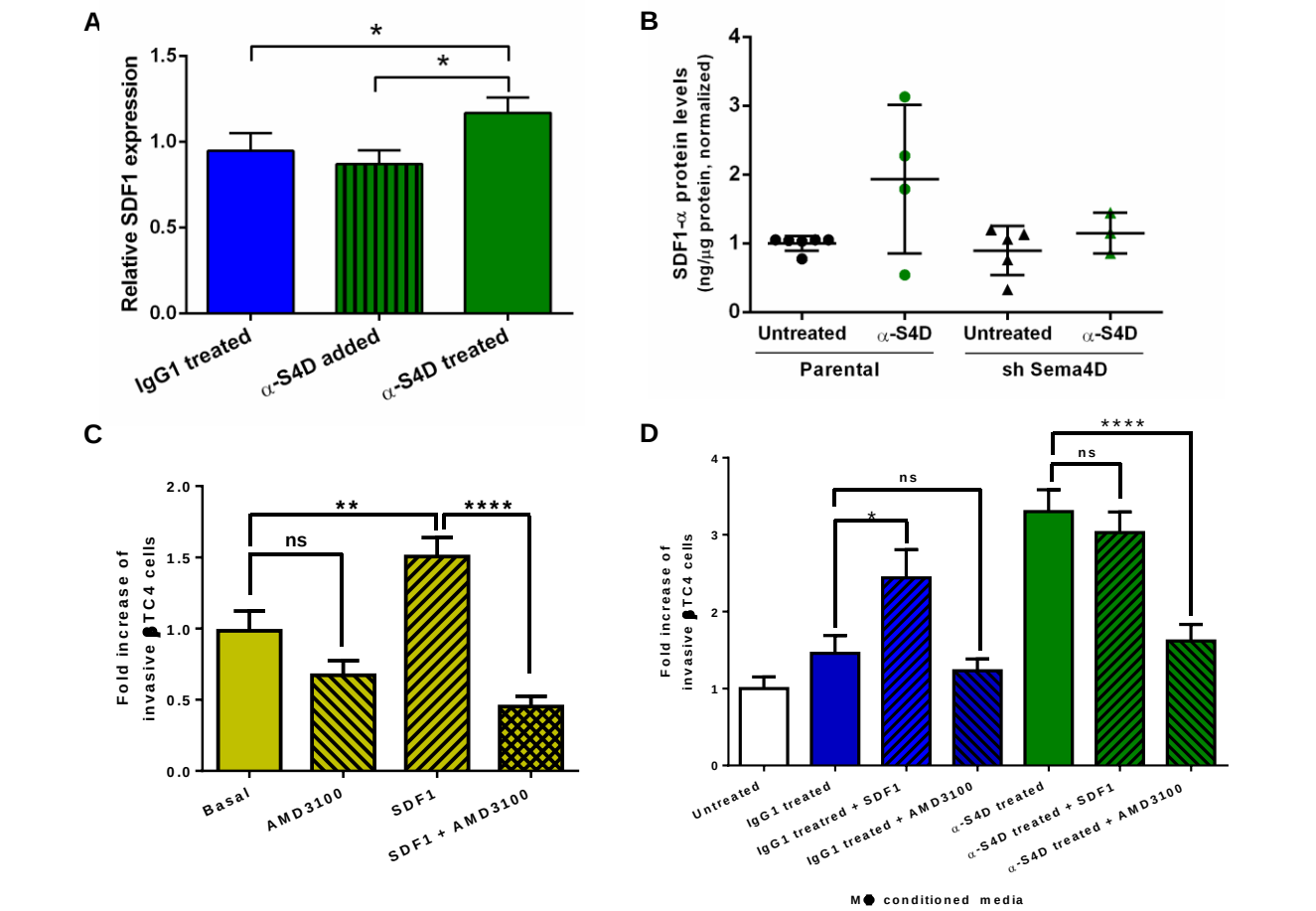

E

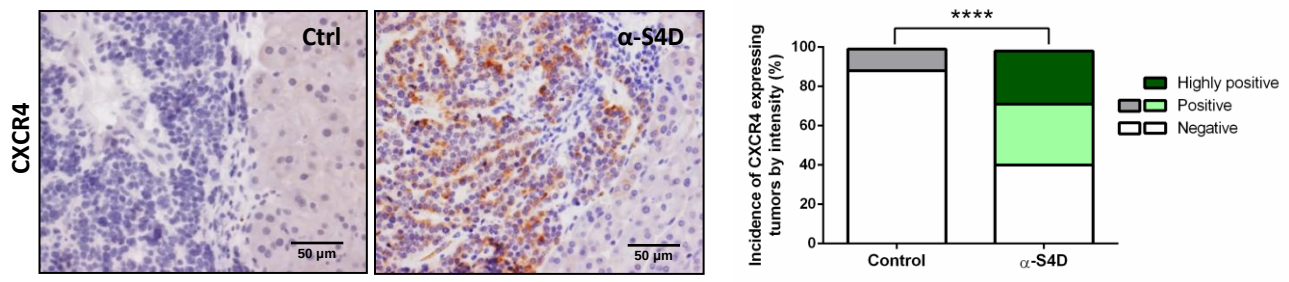

F

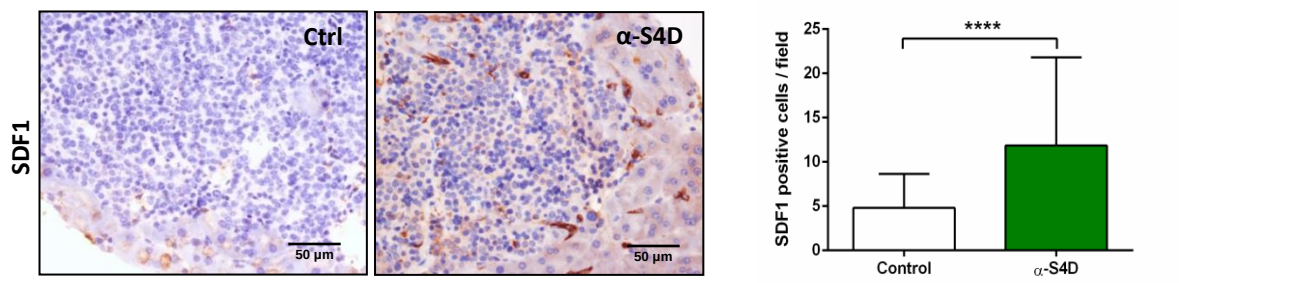

G

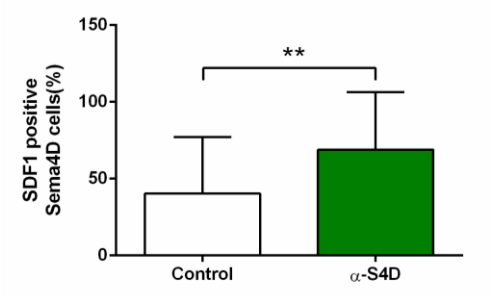

H

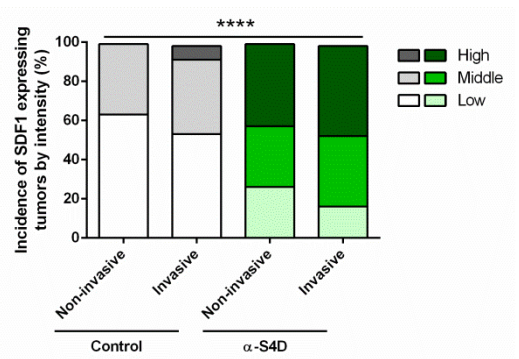

Figure 7

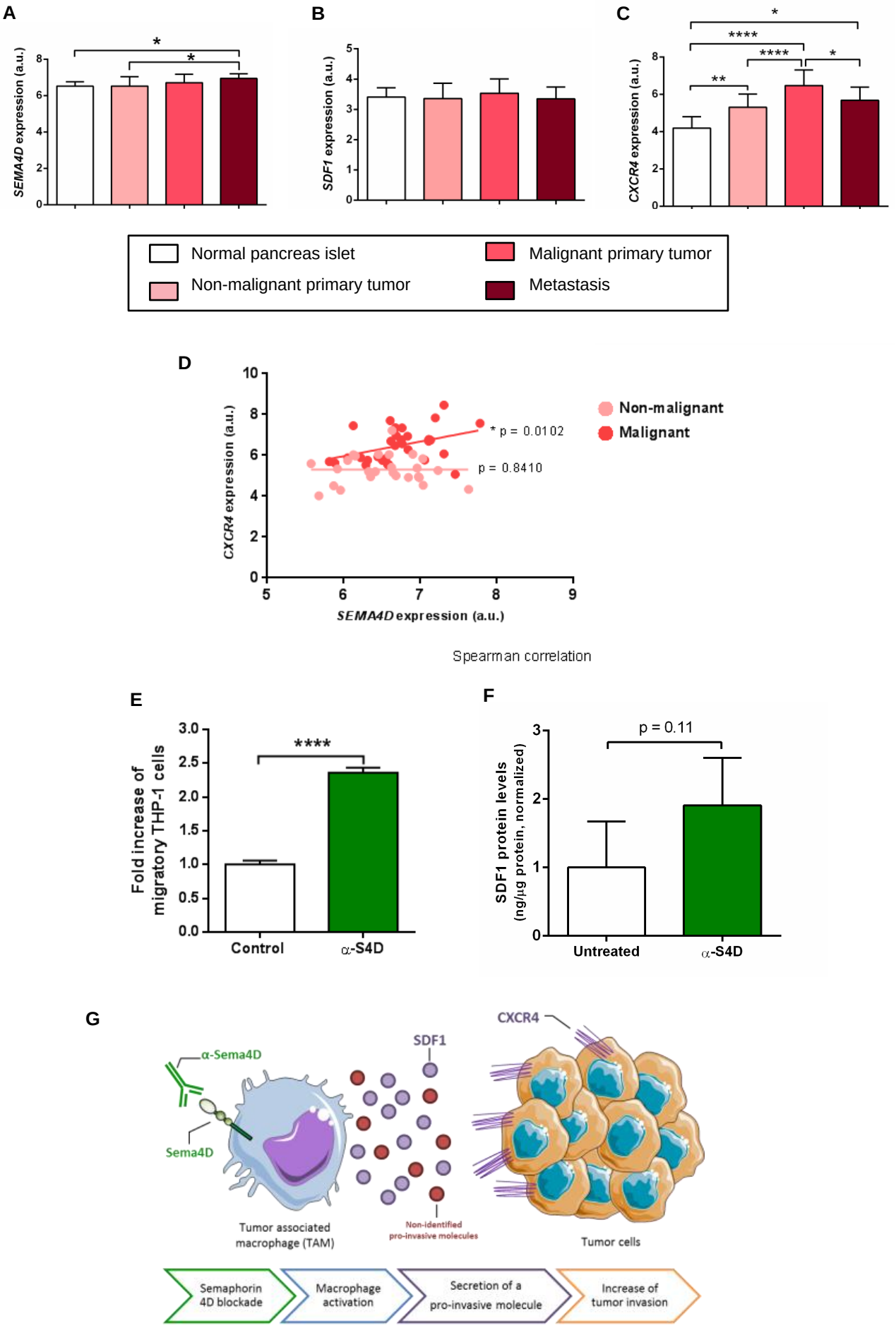
A
B
C
SEMA4D expression (a.u.)
SDF1 expression (a.u.)
CXCR4 expression (a.u.)
Normal pancreas islet
Non-malignant primary tumor
Malignant primary tumor
Metastasis
D
CXCR4 expression (a.u.)
SEMA4D expression (a.u.)
* p = 0.0102
p = 0.8410
Non-malignant
Malignant
Spearman correlation
E
Fold increase of migratory THP-1 cells
****
Control
α-S4D
F
SDF1 protein levels (ng/µg protein, normalized)
p = 0.11
Untreated
α-S4D
G
α-Sema4D
Sema4D
SDF1
CXCR4
Tumor associated macrophage (TAM)
Non-identified pro-invasive molecules
Tumor cells
Semaphorin 4D blockade
Macrophage activation
Secretion of a pro-invasive molecule
Increase of tumor invasion